Jurnal Kimia Valensi, 5(1), Mei 2019, 23-34
Available online at Website: http://journal.uinjkt.ac.id/index.php/valensi

Rapid Method for Analyzing Gadolinium Binding Activity using Colorimetric Assay Employing PAR

Metode Cepat untuk Menganalisis Aktivitas Pengikatan Gadolinium Menggunakan Uji Kolorimetri yang Melibatkan PAR

Meri Ayurini[1*], Tony Ekkelenkamp[2], Jos Paulusse[2,3], J.F.J. Engbersen[2]

[1]Chemistry Department, Universitas Pertamina, Jalan Teuku Nyak Arief, Jakarta Selatan, 12220, Indonesia
[2]Department of Biomedical Chemistry, University of Twente, Drienerlolaan 5, Enschede, 7522 NB, Netherlands
[3]Department of Biomolecular Nanotechnology, University of Twente, Drienerlolaan 5, Enschede, 7522 NB, Netherlands

[*]*Corresponding author: ayurini105@gmail.com; meri.ayurini@universitaspertamina.ac.id*

Received: September 2018; Revised: October 2018; Accepted: December 2018; Available Online: May 2019

Abstrak

Pada penelitian ini, kami mempelajari *colorimetric assay* yang melibatkan *4-(2-pyridilazo)-resorcinol* (PAR) untuk analisis kuantitatif jumlah gadolinium bebas dan yang terikat dengan ligan dalam sistem. Penelitian ini adalah studi awal untuk mengamati pola kompleksasi antara Gd^{3+} dan molekul target yang dilakukan dalam 100 mM bufer MES pH 5.5. Konstanta pengikatan (Log K) dari kompleks Gd^{3+}-PAR (1-1) pada pH 5.5 adalah 4.41 ± 0.09 M^{-1}. Karena metode ini hanya menggunakan UV-Vis Spektroskopi, disimpulkan bahwa *colorimetric assay* yang melibatkan PAR adalah metode yang cepat dan murah untuk menganalisis aktivitas pengikatan antara Gd^{3+} dan ligan target.

Katakunci: Gadolinium, *colorimetric assay*, agen pengkontras MRI.

Abstract

In this research, we study a colorimetric assay employing 4-(2-*pyridylazo*)-*resorcinol* (PAR) for quantifying the chelated and free gadolinium in the system. This is a preliminary study in order to observe the complexation behavior between Gd^{3+} and targeted molecules. This was carried out in 100 mM MES buffer at pH 5.5. The binding constant (Log K) of the Gd^{3+}-PAR (1:1) complex at pH 5.5 is 4.41 ± 0.09 M^{-1}. Since this method only uses UV-Vis spectrometry, it is concluded that colorimetric assay employing PAR is a fast and inexpensive method in order to analyze the binding activity between Gd^{3+} and targeted ligands.

Keywords*:* Gadolinium, colorimetric assay, MRI contrast agent.

DOI: *10.15408/jkv.v5i1.9238*

1. INTRODUCTION

Gadolinium is one of the lanthanides in which as a cation possesses three positive charges denoted as Gd^{3+}. It possesses seven unpaired electrons, hence it is highly paramagnetic. This property makes Gd^{3+} an excellent contrast agent for MRI. However, free gadolinium(III) ions are highly toxic (Rogosnitzky and Branch, 2016). In our body, Gd^{3+} tends to compete with Ca^{2+} since they have similar ionic radii, which are 1.05-1.11 Å and 1.00-1.06 Å, respectively (Housecroft and Sharpe, 2012; Evans, 1990). Gd^{3+} can also displace Ca^{2+} of calcium-binding enzymes owing to Gd^{3+} having higher binding affinity than calcium. As a result, all biological processes catalyzed by these enzymes are altered. (Sherry *et al.*, 2009). In effect, Gd^{3+} has to be complexed by strong organic chelators before being administrated into the body. Gadolinium-based poly(amino carboxylate)s have been widely used commercially as contrast agents for MRI

P-ISSN: 2460-6065, E-ISSN: 2548-3013

(Zhou and Lu, 2012; Lohrke *et al.*, 2016). However, the commercially available contrast agents have limitation such as rapid circulation time and low resolution of contrast enhancement (Gregorio *et al.*, 2013; Mi *et al.*, 2013). It is also reported that it can deposit to our tissues such as kidney, liver, bone, and brain (Ramalho *et al.*, 2016; Yì-Xiáng Wang *et al.*, 2015; Murata *et al.*, 2016; Darrah *et al.*, 2009). Thus, researchers have been trying to bind them by using larger molecules (Gao *et al.*, 2017). In order to do a preliminary test about the behavior of Gd^{3+} interacts with target molecules, in this research we do the study of the colorimetric assay using UV-Vis spectrophotometer. UV-Vis spectophotometer is widely used for several quantitative measurements (Biswas *et al.*, 2011; Langergraber *et al.*, 2004; Patel *et al.*, 2013). This method is based on the absorption of light in the solution. The correlation between intensity and concentration of the compound can be explained by the Lambert-Beer law. Since the colorimetric assay can only measure the concentration of the colored compound, some colorless compounds, such as colorless metals, have to be complexed by a metallochromic indicator. A metallochromic indicator is a dye compound, which has a characteristic absorption in the visible range when it is complexed with metal. In this research, we use 4-(2-pyridylazo)-resorcinol (PAR) as a metallochromic indicator which acts as a terdentate ligand, comprising of the pyridine nitrogen, *O*-hydroxyl, and a nitrogen atom of the azo bond, (Gearey *et al.*, 1962) as depicted in

Figure **1**. PAR is widely used in analytical chemistry, which has good solubility in water, and also good sensitivity and reproducibility in color (Sabel *et al.*, 2010; Genç *et al.*, 2010; Anderson and Nickless, 1967; Munshi and Dey, 1970). As a complex in particular with lanthanides, stoichiometries between PAR and the lanthanides of 2 : 1 or 1 : 1 have been reported (Munshi and Dey, 1970; Ohyoshi, 1984).

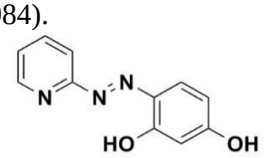

Figure 1. Structure of PAR

Thus in this research we used colorimetric assay employing PAR in order to find a rapid and simple method to analyze the binding activity between Gd^{3+} and targeted ligand. Aside from complexation study, the best conditions for gadolinium solutions were also determined.

2. MATERIALS AND METHODS

Materials and Instrumentation

Materials used in this research were gadolinium(III) chloride hexahydrate ($GdCl_3$•$6H_2O$; Sigma Aldrich, 99%), 4-(2-pyridylazo)-resorcinol (PAR; Sigma Aldrich), diethylenetriaminepentaacetic acid (DTPA; Sigma Aldrich, ≥ 99 %), 1,4,7,10-tetraazacyclododecane-1,4,7,10-tetraacetic acid (DOTA; Sigma Aldrich, 97.0 %), ethylenediamine-N,N'-diacetic acid (EDDA; Sigma Aldrich, ≥ 98 %), HEPES (Sigma Aldrich), glycine (Merck-Schuchardt), MES monohydrate (Sigma Aldrich), dimethyl sulfoxide (DMSO; Biosolve), and milli-Q water which was free from any metals (after adding chelex 100, Sigma Aldrich). While UV-Vis spectrophotometer (Carry 300 UV-Vis) was used as instrumentation.

Procedures

Solubility and Stability of Gadolinium solutions in Several Buffers

50 mM glycine buffer (pH 10), 10 mM HEPES buffer (pH 7.4), and 100 mM MES buffer (pH 5.5) were prepared. The pH was adjusted with 4 M NaOH and 4 M HCl. Gd^{3+} solutions were prepared by dissolving $GdCl_3$•$6H_2O$ in the aforementioned buffers. The solubility and the stability of gadolinium solution in these buffers with different pH were observed by UV-Vis spectrometry (Carry 300 UV-Vis) employing PAR. The stock solutions of PAR in two buffers (HEPES pH 7.4 and MES pH 5.5) were prepared by dissolving 2.2 mg of PAR in 5 mL DMSO and diluted with the buffers separately in 50 mL volumetric flask to obtain 200 µM of PAR in solutions. Afterward, the 200 µM PAR were diluted to 20 µM and 40 µM in HEPES and MES buffers, respectively. The Gd^{3+} solutions (200 µM) were prepared in both HEPES and MES buffers and incubated for 0.5 h, 1 h, 2 h, 3 h, and 6 h at room temperature (RT). The UV-Vis spectra of the solutions containing 10 µM PAR and 100 µM Gd^{3+} (pH 7.4 HEPES buffer) and 20 µM PAR and 100 µM Gd^{3+} (pH 5.5 MES buffer) were recorded in the range of 350 – 650 nm.

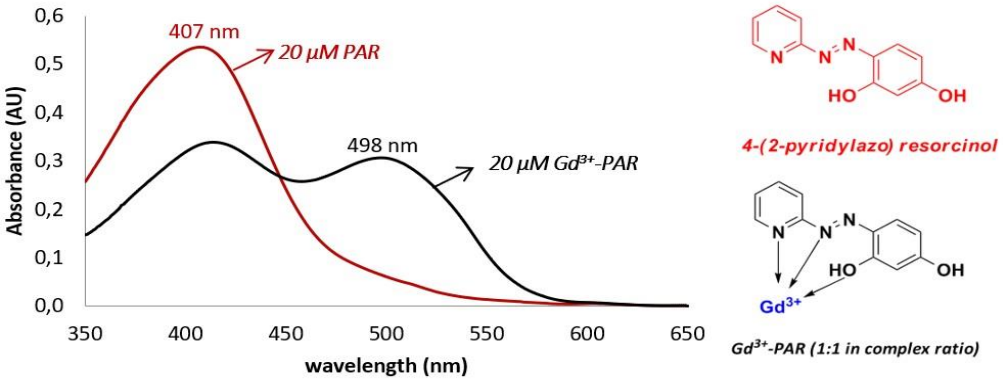

Figure 2. UV-Vis spectra of free PAR and Gd^{3+}-PAR complex in 100 mM MES Buffer (pH 5.5). Red line = 4-(2-pyridylazo) resorcinol and black line = gd3+-PAR (1:1 complex ratio).

UV-Vis Spectra of Gd^{3+}-PAR Complex

UV-Vis spectra of Gd^{3+}-PAR complex (Gd^{3+} concentration range: 0-3200 µM) containing 15 data points were measured in 100 mM MES buffer (pH 5.5) by using UV-Vis spectroscopy (Carry 300 UV-Vis) in disposable cuvettes with 1 cm path length. In this measurement, MES buffer pH 5.5 was used as a blank. 0.6 mL of PAR 40 µM and 0.6 mL of Gd^{3+} solutions (concentration range: 0-6400 µM) were mixed. Afterward, their UV-Vis spectra were recorded in the range of 355-650 nm. All measurements were done in triplicate.

Ligand Competition Experiment

Firstly, the UV-Vis spectra of mixed Gd^{3+} and ligand solutions were recorded in the range of 350-650 nm to verify that the formed Gd^{3+}-ligand complex will not have any absorption at that range. In order to study the behavior of Gd^{3+}-PAR complex in the presence of the other ligands, the experiment as follows was carried out. Four solutions containing contained PAR (20 µM), Gd^{3+} (a.50, b.100, c.160, d. 200 µM), and ligand (50 µM) were prepared. Afterward, the UV-Vis spectra of them were recorded by UV-Vis spectroscopy in the range of 350-650 nm. All measurements were done in duplicate. Furthermore, the similar experiment as just described previously was carried out to estimate the binding constants and the binding capacities of Gd^{3+} in the ligands (DTPA, DOTA, and EDDA). The final concentrations of PAR, $Gd^{3+,}$ and ligands in this experiment are PAR (20 µM), Gd^{3+} (25, 50, 100 µM), and Ligand (25, 50, 100 µM).

3. RESULTS AND DISCUSSION

Complexation Study of Gadolinium by Colorimetric Assay

Complexation studies of gadolinium were carried out in order to determine both chelated and free gadolinium concentrations in the system. Furthermore, this study is expected to find a simple method to observe the complexation behavior between Gd^{3+} and targeted molecules. This was carried out by colorimetric assay employing PAR as a metallochromic indicator. This assay based on UV-Vis spectroscopy was chosen, because it is a relatively inexpensive technique thus more simple as compared to other techniques, such as ICP-MS. In the beginning, solubility and stability of gadolinium solutions in several pH and buffers was observed in order to determine the best conditions to do this study. Afterward, the complexation of Gd^{3+} and PAR with and without combination of several ligands (DTPA, DOTA, and EDDA) was evaluated in this study.

Figure **2** shows the UV-Vis spectra of PAR without Gd^{3+} and PAR completely complexed with Gd^{3+} in 100 mM MES Buffer at pH 5.5. The structures of uncomplexed and 1:1 ratio complexed PAR with Gd^{3+} also are displayed close to the UV-Vis spectra. The maximum absorption of free PAR in solution is at 407 nm. A new peak at 498 nm indicates the presence of Gd^{3+}-PAR complex.

Solubility and Stability of Gadolinium Solutions in Several Buffers

The solubility and stability of gadolinium (III) solution are important to be known before the further complexation study

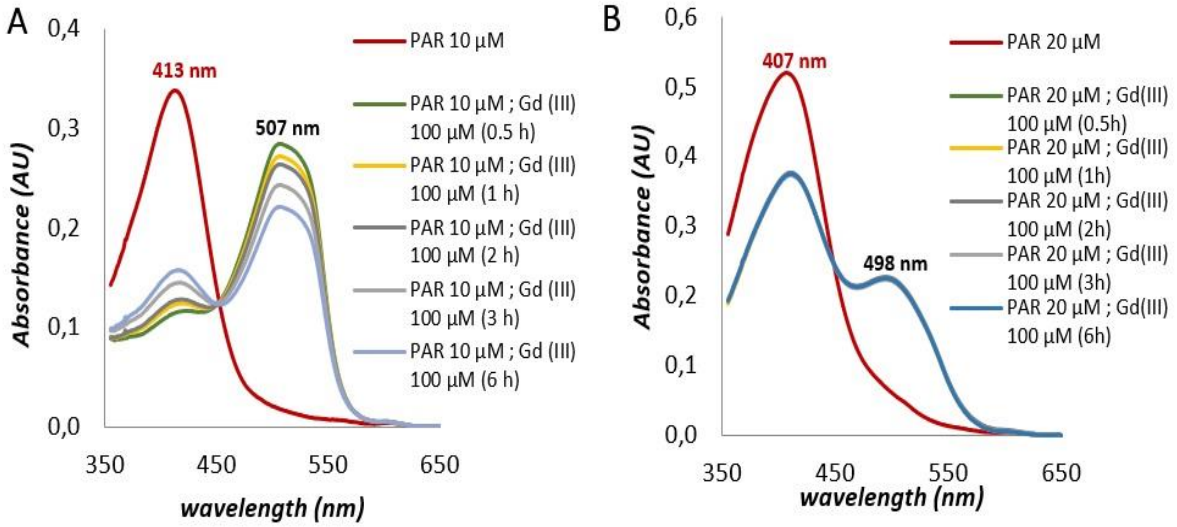

Figure 3. UV-Vis spectra of Gd^{3+}-PAR complex: **A)** in 10 mM HEPES buffer (pH 7.4); **B)** In 100 mM MES buffer (pH 5.5) after the Gd^{3+} solution incubation (0.5 h - 6 h) at RT.

of the gadolinium itself. The solubility of gadolinium relies on the pH of the solutions. In glycine buffer at pH 10, gadolinium at concentration of 64 – 3200 µM already resulted in precipitation, which was presumably caused by the formation of gadolinium hydroxide ($Gd(OH)_3$). $Gd(OH)_3$ is insoluble in water. However, in HEPES buffer at pH 7.4 and in MES buffer at pH 5.5 (acidic conditions), no precipitation was observed when gadolinium at aforementioned concentrations was added. To verify the latter observation, the stabilities of the gadolinium solutions in either HEPES buffer (pH 7.4) or MES buffer (pH 5.5) were measured by UV-Vis spectroscopy technique with PAR as the metallochromic indicator. In this case, the stability is defined as whether the UV-Vis spectra of solutions containing Gd^{3+} and PAR change or not when the Gd^{3+} solution used is incubated at room temperature for a period of time. Figure 3A and 3B represent the UV-Vis spectra of PAR in the presence of the Gd^{3+} solutions in some period of time in respective HEPES Buffer at pH 7.4 and MES Buffer at pH 5.5. Figure 3A, where the absorbance of Gd^{3+}-PAR complex decreased after period of Gd^{3+} solutions incubation (0.5–6 h), indicates that the gadolinium was not stable in HEPES buffer at pH 7.4. The lowered stability was caused by the formation of $Gd(OH)_3$. This has occurred since the pH of the solution was 7.4, and consequently contained an excess amount of hydroxide ions. Although no precipitation was observed during the experiment, most likely very small amounts of $Gd(OH)_3$ formed under these conditions. Figure 3B shows no significant change in the UV-Vis spectra (all spectra of solutions containing PAR and Gd(III) overlap). It indicates that the gadolinium solutions were stable in MES buffer at pH 5.5. Based on these results, the proceeding experiments with gadolinium were carried out in MES buffer (pH 5.5).

UV-Vis Spectra, Calibration Curve, and Binding Constant Determination of Gd^{3+}-PAR Complex

The UV-Vis spectra of PAR (20 µM) containing various concentrations of gadolinium (0-3200 µM) in the range of 350-650 nm as shown in Figure 4. In this case, the free Gd^{3+} solution was observed to display no absorption in the aforementioned wavelength range (spectrum not shown). The maximum intensity of the PAR absorption at 407 nm decreased upon addition of gadolinium(III) ion. The new peak that appears at 498 nm indicates the formation of the Gd^{3+}-PAR complex, of which the absorbance increases upon increasing the Gd^{3+} concentration. The presence of an isosbestic point at 447 nm indicates that two species (PAR and Gd^{3+}-PAR complex) are at equilibrium and no interfering species were formed during the reaction.

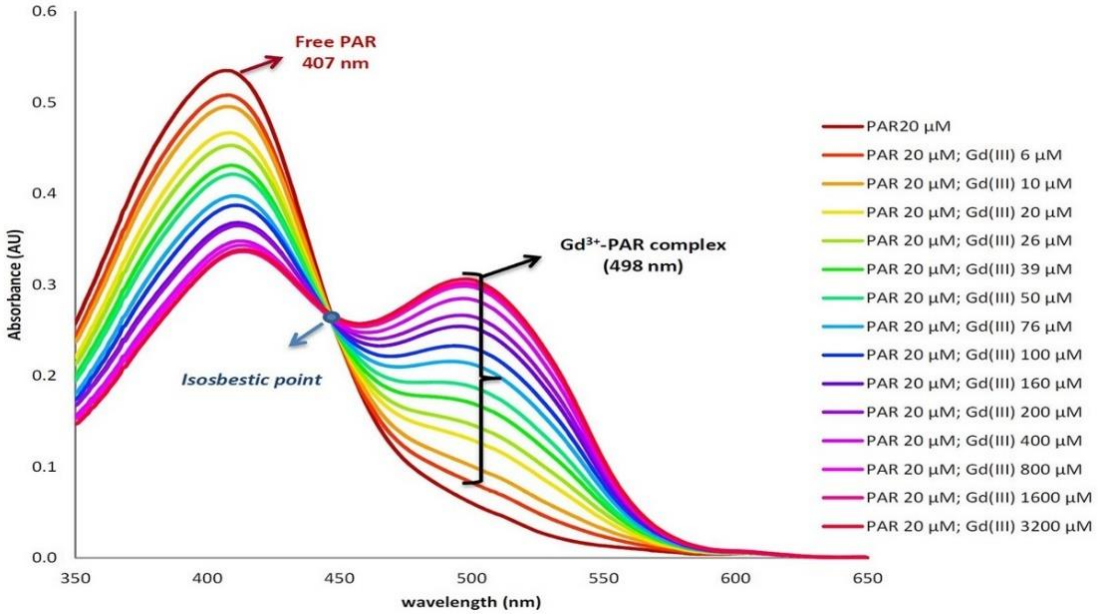

Figure 4. UV-Vis Spectra of PAR and Gd^{3+}-PAR complexes at various concentration of Gd^{3+} solutions in 100 mM MES Buffer (pH 5.5)

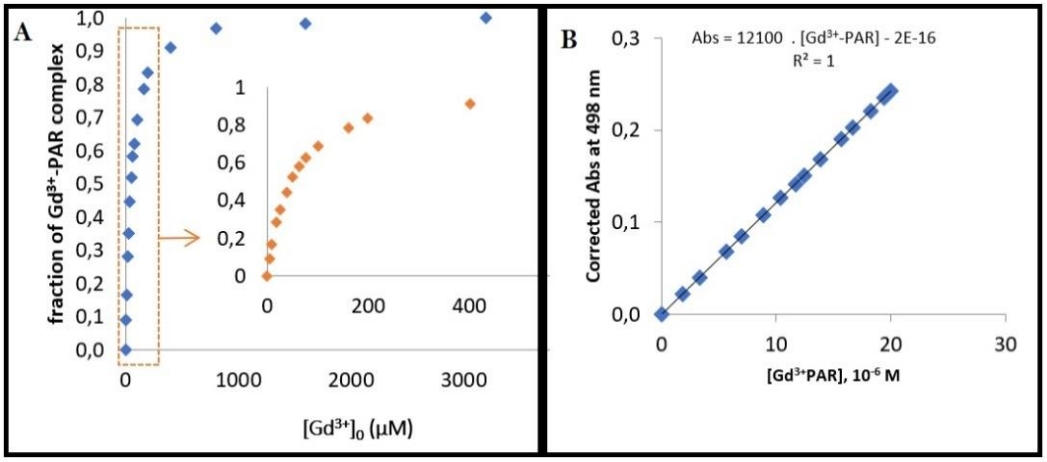

Figure 5. A) Fraction of Gd^{3+}-PAR complex versus initial Gd^{3+} concentrations (0-3200 µM $[Gd^{3+}]_o$); B) Corrected absorbance at 498 nm versus concentration of Gd^{3+}-PAR complex in order to determine the molar extinction coefficient of the complex

According to the UV-Vis spectra shown in Figure 4, PAR without Gd^{3+} present displays a minor absorption (at 498 nm) of 0.063 ± 0.002 denoted as A_o. Moreover, when the initial concentration of gadolinium (3200 µM) was much higher than the concentration of PAR (20 µM), the absorbance at 498 nm was 0.306 ± 0.002, defined as A_{max}. It is assumed that all PAR is complexed with Gd^{3+}. The fraction of the formed complex then can be calculated using equation 1.1, where A is the absorbance of the complex at 498 nm in the range of A_0 until A_{max}.

The correlation between the fraction of the formed complex and the initial gadolinium concentrations is shown in

Figure **5**A. This fraction increases considerably up to 200 µM of initial Gd^{3+} concentration, then it only increases slightly and remains constant. According to the data points in the

Figure **5**A and the assumption that the ratio of Gd^{3+} and PAR in the complex is 1:1 (if $[Gd^{3+}]$ >>, the $[Gd^{3+}\text{-PAR}]_{max} = [PAR]_0$), thus the concentration of the formed Gd^{3+}-PAR complex in different initial concentration of Gd^{3+} can be calculated by using equation 1.2.

$$fraction\ of\ (Gd^{3+}\text{–}PAR)\ complex\ = \frac{(A - A_0)}{(A_{max} - A_0)} \quad (1.1)$$

$$[Gd^{3+}\text{–}PAR]_{eq} = \frac{(A - A_0)}{(A_{max} - A_0)} \times [PAR]_0 \quad (1.2)$$

$$Gd^{3+} + PAR \underset{}{\overset{K}{\rightleftharpoons}} Gd^{3+}\text{-}PAR \quad (1.3)$$

$$K = \frac{[Gd^{3+}\text{–}PAR]_{eq}}{([PAR]_0 - [Gd^{3+}\text{–}PAR]_{eq}).\ ([Gd^{3+}]_0 - [Gd^{3+}\text{–}PAR]_{eq})} \quad (1.4)$$

$$[Gd^{3+}]_{eq} = [Gd^{3+}]_0,\ \text{assume:}\ [Gd^{3+}]_0 >> [Gd^{3+}\text{–}PAR]_{eq} \quad (1.5\ A)$$

$$[Gd^{3+}]_{eq} = [Gd^{3+}]_0 - [Gd^{3+}\text{–}PAR]_{eq} \quad (1.5\ B)$$

$$\frac{(A - A_0)}{(A_{max} - A)} = K.[Gd^{3+}]_0 \quad (1.6\ A)$$

$$\frac{(A - A_0)}{(A_{max} - A)} = K.[Gd^{3+}]_{eq} \quad (1.6\ B)$$

Furthermore, the molar extinction coefficient (Ɛ) of the Gd^{3+}-PAR complex was determined by plotting the curve of corrected absorbance at 498 nm indicating formation of Gd^{3+}-PAR complex towards the concentrations of formed complex. That curve is shown in

Figure 5B. The slope of the curve is the Ɛ of Gd^{3+}-PAR complex based on the Lambert-Beer law ($A = Ɛ \bullet b \bullet C$) in $M^{-1}\ cm^{-1}$. The Ɛ of Gd^{3+}-PAR complex obtained by this work is $1.21 \times 10^4\ M^{-1}\ cm^{-1}$, which is in agreement with the literature (Ohyoshi, 1984). Moreover, the calibration curve of Gd^{3+} and the binding constant of Gd^{3+}-PAR complex were derived from equilibrium reaction 1.3. According to this equilibrium reaction, the correlation between binding constant of Gd^{3+}-PAR complex (K) and the $[Gd^{3+}]_0$, $[PAR]_0$, $[Gd^{3+}\text{-PAR}]$ can be seen in equation 1.4.

Regarding with equation 1.4, there are two approximations to simplify, which are displayed in equation 1.5 A and 1.5 B, respectively. The first approximation was obtained by neglecting the $[Gd^{3+}\text{-PAR}]_{eq}$ towards the $[Gd^{3+}]_0$. The second one, by rewriting the $[Gd^{3+}]_0$ - $[Gd^{3+}\text{-PAR}]_{eq}$ being $[Gd^{3+}]_{eq}$ without changing the meaning.

In literature reported by Benesi and Hildebrand (1949), the first approximation was chosen. In this study, both approximations are used and compared. By substituting equation 1.2 in equation 1.4 in both approximations, the new equations (equation 1.6 A and 1.6 B) are obtained for respective approximations.

According to the equation 1.5 A and 1.5 B, the calibration curves in respective approximations were constructed, which are shown in Figure 6A and Figure 6B, respectively. The straight lines (R^2 = 0.99) of the two calibration curves, which are constructed based on the equation derived by the assumption that the ratio of PAR and Gd^{3+} is 1:1, confirm that the assumption (1:1) is true. Then, the calibration curves will be used to determine the binding constant of Gd^{3+}-PAR complex and the concentration of unbound gadolinium (III) ion in the system.

The binding constant of Gd^{3+}-PAR complex (K in M^{-1}) is the slope of the curve in Figure 6. In logarithmic form (Log K), they are $4.41 \pm 0.09\ M^{-1}$ and $4.43 \pm 0.09\ M^{-1}$, respectively. The deviation (± 0.09) was obtained from the measurements which were done in triplicate. The results show no significant difference in the binding constant of Gd^{3+}-PAR complex. Thus, these two approximations can be used to determine the binding constant of Gd^{3+}-PAR complex. These results are similar to the formation constant of protonated 1:1 complex between PAR and Gd^{3+} in pH 5-6 ($\log K_{GdHPAR} = 4.28 \pm 0.03\ M^{-1}$) reported by Ohyoshi (1984). However, Oyoshi also reported the observation of unprotonated complex which has Log K_{GdPAR} of $10.25 \pm 0.07\ M^{-1}$.

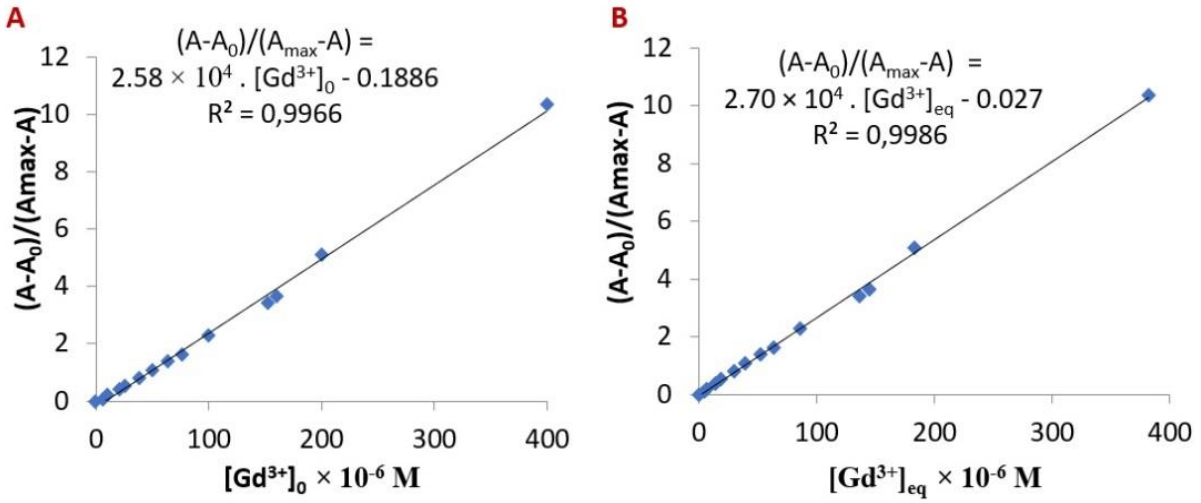

Figure 6. Calibration curve of Gd^{3+}: A) first approximation which neglects the $[Gd^{3+}\text{-PAR}]_{eq}$ towards the $[Gd^{3+}]_0$, B) second approximation which $[Gd^{3+}]_{eq} = [Gd^{3+}]_0 - [Gd^{3+}\text{-PAR}]_{eq}$

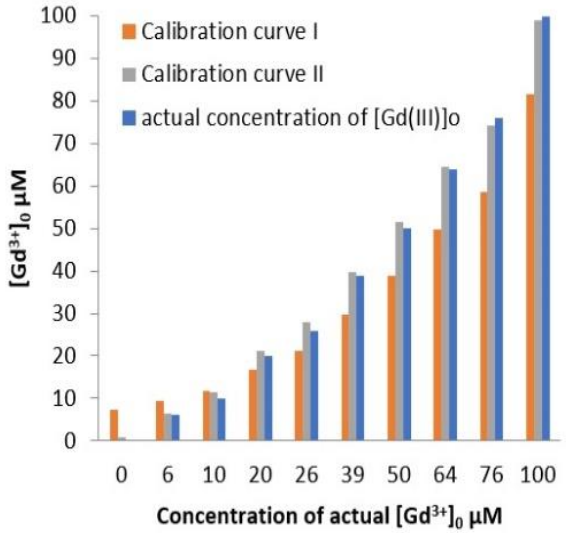

Figure 7. Comparison of the initial gadolinium (III) concentrations according to calibration curve I, calibration curve II, and their actual concentrations

For determination of bound and unbound Gd^{3+} in the solutions, these two calibration curves (Figure 6) give quite large differences. When the equations of those two calibration curves are used to recalculate the concentration of $[Gd^{3+}]_0$, the error given by the first calibration curve is larger than the second calibration curves, in particular at the range of 0 – 100 µM $[Gd^{3+}]_0$ (

Figure **7**). This means that neglect the concentration of Gd^{3+}-PAR complex towards the initial concentration of Gd^{3+} (First approximation) is not good approximation in this case. Thus, we used the second calibration curve for the determination of both bound and unbound Gd^{3+} in the ligand competition experiments.

The Behavior of Gd^{3+}-PAR Complex in Presence of The Other Ligands, Binding Constants, and Binding Capacities of Gd^{3+} in Several Ligands

The behavior of Gd^{3+}-PAR complex in the presence of the other competing ligands was studied spectrophotometrically through ligand competition experiments. In this study, the binding constants and the binding capacities of Gd^{3+} with several ligands was estimated. Here, PAR and the ligands will compete to form complexes with Gd^{3+}. The employed ligands in this study were DTPA, DOTA, and EDDA, of which the structures are depicted in Figure 8. No absorptions in the UV-Vis wavelength range were observed for solutions of these three ligands. Furthermore, the mixed solutions containing Gd^{3+} and these three ligands separately also showed no absorptions in the UV-Vis range. Hence, the observed absorption at 498 nm is only caused by Gd^{3+}-PAR complex.

The results of the ligand competition experiments are displayed in

Figure **9**. The fraction of formed Gd^{3+}-PAR complex in the absence and presence of the ligands (DTPA, DOTA, or EDDA) at several initial concentrations of Gd^{3+} solutions is depicted. In these experiments, both the concentrations of PAR and the ligands were kept constant, which were 20 µM and 50 µM,

respectively. Meanwhile, the concentrations of initial Gd^{3+} increased from 50 µM until 200 µM. According to these data, it was observed that the presence of the ligands reduces the fraction of the Gd^{3+}-PAR complex. This means that the presence of these ligands shifts the equilibrium of PAR and Gd^{3+} in order to form Gd^{3+}-PAR complex to the reactants. In the competition experiment, the equilibrium between PAR, Gd^{3+}, and ligand can be seen in equilibrium **1.7**.

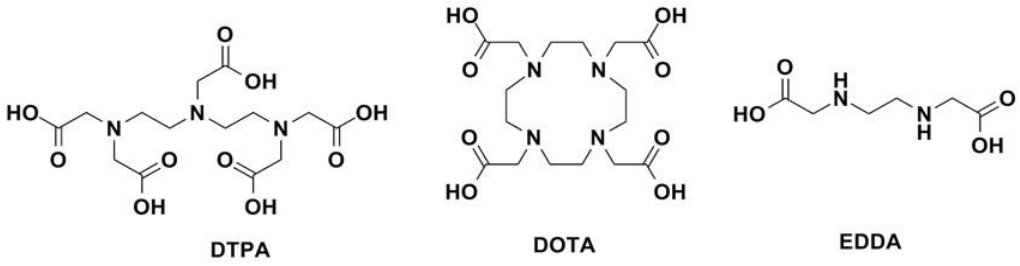

Figure 8. Structures of DTPA (L1), DOTA (L2), and EDDA (L3)

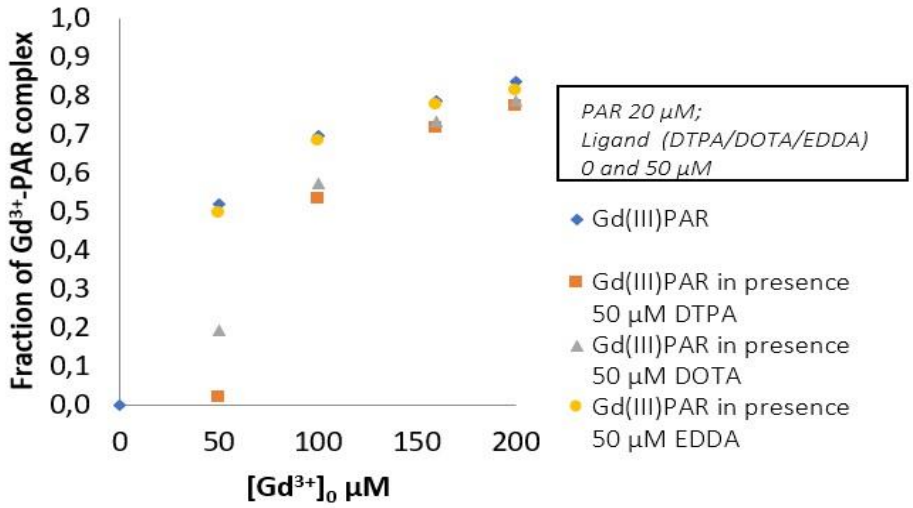

Figure 9. Fraction of Gd^{3+}-PAR complex in the presence of competing ligands

$$\begin{array}{l} \mathbf{PAR + Gd^{3+} \overset{K}{\rightleftharpoons} Gd^{3+}\text{-}PAR} \\ \quad + \\ \mathbf{Ligand} \\ \quad \Big\Updownarrow K_L \\ \mathbf{Gd^{3+}\text{-}Ligand} \end{array} \qquad (1.7)$$

Furthermore, the data obtained in the ligand competition experiments are displayed by plotting the curves (

Figure **10**), which are similar to the first calibration curve as described in Figure 6A. This is in order to give more obvious observation regarding equilibrium 1.7. Here, the slopes of the curves are the binding constants of Gd^{3+}-PAR in the absence and presence of the competing ligands.

Moreover, according to the

Figure **10**, it is observed that DTPA and DOTA give much reduction of the formed Gd^{3+}-PAR complex and the trend tends to be constant. This indicates that DTPA and DOTA have binding constants that are much higher than PAR and full competition with PAR occurs. On the other hand, EDDA only gives a small reduction. It indicates that the binding constant of EDDA is approximately the same with PAR. The further proof of this behavior can be seen by the results of the ligand competition experiments when the concentration of Gd^{3+} and the ligands were the same in the fixed concentration of PAR (20 µM). The results are shown in Tabel 1.

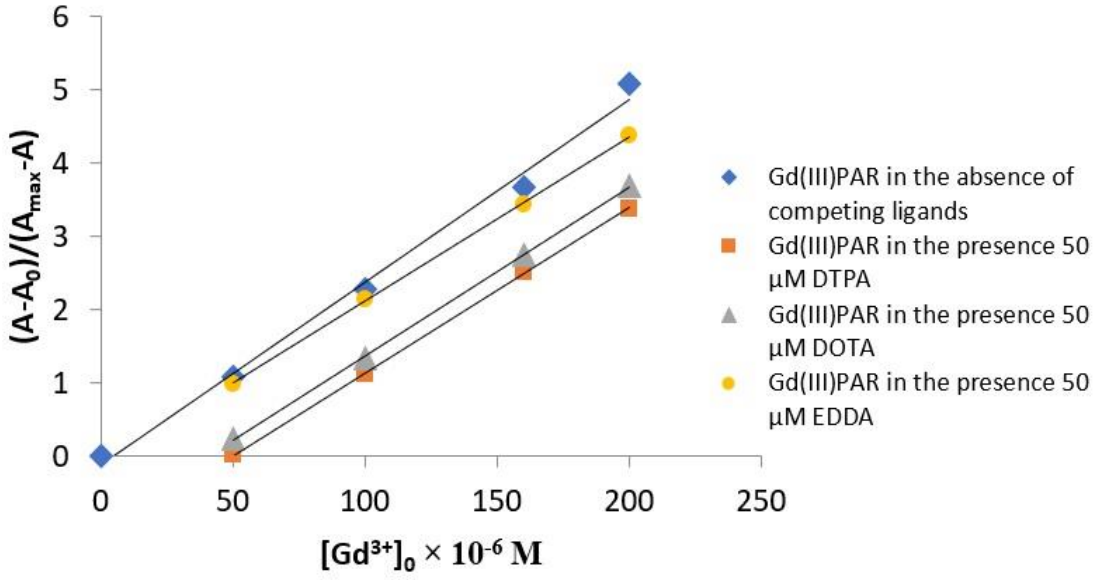

Figure 10. $(A-A_0)/(A_{max}-A)$ versus $[Gd^{3+}]_0 \times 10^{-6}$ M^{-1} of Gd^{3+}-PAR complex before and after ligand competition experiments

Table 1. Results of ligand competition experiments for determination of binding capacities and binding constants of Gd^{3+} in several ligands

$[Gd^{3+}]_0$ µM	$[Ligand]_0$ µM	$[Gd^{3+}\text{-}PAR]_{eq}$ µM	$[Gd^{3+}]_{eq}$ µM	$[Gd^{3+}\text{-}Ligand]_{eq}$ µM	$[Ligand]_{eq}$ µM	Binding capacity %	Log K	Log K in Average
	DTPA							
25	25	0.17	1.31	21.52	1.48	94	7.08	
50	50	0.35	1.66	47.99	2.01	96	7.15	7.04 ± 0.13
100	100	1.03	3.01	95.96	4.04	96	6.89	
	DOTA							
25	25	2.09	5.33	17.58	7.42	70	5.65	
50	50	1.86	9.87	36.27	11.73	72	5.43	5.36 ± 0.32
100	100	7.43	22.92	69.65	30.35	70	5.00	
	EDDA							
25	25	6.43	18.57	0	25.00	0	-	
50	50	9.95	37.65	2.40	47.60	5	1.13	1.23 ± 0.14
100	100	11.22	71.18	11.60	86.40	14	1.33	

The concentration of Gd^{3+}-PAR complex at equilibrium in these ligand competition experiments was calculated by using equation 1.2. Meanwhile, the unbound Gd^{3+} in equilibrium can be determined by using the calibration curve shown in Figure 6B. The second calibration curve is preferred to be used owing to the lower error as compared to the first calibration curve as explained before. Furthermore, the concentration of Gd^{3+}-ligand and ligand at equilibrium can be calculated by using equation 1.8 and 1.9, respectively.

The binding capacities (BC) of the several ligands to bind Gd^{3+} were calculated by using equation 1.10. Moreover, the binding constants of Gd^{3+}-ligand were calculated by equation 1.11, which was derived from the equilibrium reaction 1.7 as just described previously.

$$[Gd^{3+}\text{–Ligand}]_{eq} = [Gd^{3+}]_0 - [Gd^{3+}]_{eq} - [Gd^{3+} - PAR]_{eq} \quad (1.8)$$

$$[Ligand]_{eq} = [Ligand]_0 - [Gd^{3+} - Ligand]_{eq} \quad (1.9)$$

$$BC\ (\%) = \frac{[Gd^{3+}\text{–Ligand}]_{eq}}{[Ligand]_0}.\ 100\ \% \quad (1.10)$$

$$K_L = \frac{[Gd^{3+}-Ligand]_{eq}}{[Gd^{3+}]_{eq}.\ [Ligand]_{eq}} \quad (1.11)$$

According to the data shown in **Table** 1, the binding capacities of both DTPA and DOTA tend to constant when the concentration of Gd^{3+} and Ligand (DTPA or DOTA) were doubled, which are in the range of 94 - 96 % and 70 - 72 %, respectively. This indicates that DTPA and DOTA have much higher binding constants with Gd^{3+} as compared to PAR. In the literature reported by Caravan et al, (1999), Log K_L of Gd^{3+}-DTPA and Gd^{3+}-DOTA were 22.46 and 25.3, respectively. As a result, the binding capacities of both DTPA and DOTA should be almost 100 %. For DTPA, this is indeed the case. Unfortunately, DOTA shows lower binding capacities than expected. In the experiment employing DOTA, any possibility of contamination with metals, such as from glassware and Milli-Q water, was minimalized. Thus, this unexpected result is most likely occurred due to impurities in the DOTA used. Regarding the binding constant determination of Gd^{3+} in very strong ligands, such as DTPA and DOTA, unfortunately, this method cannot be used accurately. In this method, the binding constants (Log K_L) of Gd^{3+}-DTPA and Gd^{3+}-DOTA are 7.04 ± 0.13 M^{-1} and 5.36 ± 0.32 M^{-1}, respectively. However, different behavior was observed for EDDA. The binding capacity of EDDA to bind Gd^{3+} was not constant but rather depended on the concentration of PAR and Gd^{3+}. The binding capacity of EDDA to bind Gd^{3+} increased in increasing of concentration both EDDA and Gd^{3+}. This shows that EDDA is markedly different from DTPA and DOTA that have very high binding constants with Gd^{3+}. When the concentrations of PAR (20 µM) and EDDA (25 µM) were almost the same, no Gd^{3+}-EDDA complex formation could be detected by UV-Vis spectroscopy. Furthermore, when the concentration of EDDA is twice that of PAR, the concentration of the formed Gd^{3+}-EDDA complex is still lower than Gd^{3+}-PAR as well as their binding capacities. This behavior indicates that EDDA is by far not strong enough to bind Gd^{3+} as compared to PAR. It means that as a ligand for Gd^{3+}, PAR is stronger than EDDA. According to the ligand competition experiment, the binding constant (Log K_L) of Gd^{3+}-EDDA is 1.23 ± 0.14 M^{-1}, which is lower than the binding constant of Gd^{3+}-PAR (4.41 ± 0.09 M^{-1}).

4. CONCLUSION

In this research, we have demonstrated that colorimetric assay employing PAR is a fast and inexpensive method in order to monitor the complexation between Gd^{3+} and several ligands. MES buffer (100 mM) at pH 5.5 was found out as the best condition to do the complexation study by the colorimetric assay. This method can be used to estimate the concentration of bound and unbound Gd^{3+} in the system. Furthermore, it also can monitor whether the ligand is strong or not to bind Gd^{3+}. If the binding capacity of the ligand to bind Gd^{3+} tends to be constant when the concentrations of both Gd^{3+} and the ligand are increased, this indicates that the ligand strongly binds to Gd^{3+}. Conversely, the ligand does not strongly bind Gd^{3+} if the binding capacity is not constant and tends to increase when the concentrations of both Gd^{3+} and ligand are increased.

ACKNOWLEDGEMENTS

I would like to give my gratitude to both Direktorat Jenderal Pendidikan Tinggi (DIKTI) Indonesia via Beasiswa Unggulan program and University of Twente via UT Scholarship for giving me the scholarship during my study in University of Twente.

REFERENCES

Anderson R, Nickless G. 1967. Heterocyclic azo dyestuffs in analytical chemistry. *Analyst.* 92(1093): 207-238.

Benesi H, Hildebrand J. 1949. A spectrophotometric investigation of the interaction of iodine with aromatic hydrocarbons. *Journal American Chemical Society*. 71(8): 2703-2707.

Biswas A, Sahoo J, CHatli M. 2011. A simple UV-Vis spectrophotometric method for determination of β-carotene content in raw carrot, sweet potato and supplemented chicken meat nuggets. *LWT-Food Science and Technology*. 44(8): 1809-1813.

Caravan P, Ellison JJ, McMurry TJ, Lauffer RB. 1999. Gadolinium(III) chelates as MRI contrast agents. *Chemical Reviews*. 99(9): 2293–2352.

Darrah T, Prutsman-Pfeiffer J, Poreda R, Ellen CM, Hauschka P, Hannigan R. 2009. Incorporation of excess gadolinium into human bone from medical contrast agents. *Metallomic*. 1(6): 479–488.

Evans CH. 1990. *Biochemistry of the Lanthanides*. New York(USA): Springer.

Gao L, Zhou J, Yu J, Li Q, Liu X, Sun L, Peng T, Wang J, Zhu J, Sun J, Lu W, Yu L, Yan Z, Wang, Y. 2017. A novel Gd-DTPA-conjugated poly(L-γ-glutamyl-glutamine)-paclitaxel polymeric delivery system for tumor theranostics. *Scientific Reports*, 7(1): 3799.

Gearey W, Nickless G, Polland F. 1962. The metal complexes of some azo and azomethine dyestuffs : Part I. Spectra in water, and in dioxan/water in the wavelength range 320-600 mμ. *Analytica Chimica Acta*. 26: 575-582.

Genç F, Gavazov K, Türkyilmaz M. 2010. Ternary complexes of vanadium(IV) with 4-(2-pyridylazo)-resorcinol (PAR) and ditetrazolium chlorides (DTC). *Open Chemistry*. 8(2). 461-467.

Gregorio ED, Gianolio E, Stefania R, Barutello G, Digilio G, Aime S. 2013. On the fate of MRI Gd-based contrast agents in cells. Evidence for extensive degradation of linear complexes upon endosomal internalization. *Analytical Chemistry*. 85(12): 5627-5231.

Housecroft CE, Sharpe AG. 2012. *Inorganic Chemistry* (4th ed.). London(UK): Pearson Prentice Hall.

Langergraber G, Fleischmann N, Hofstaedter F, Weingartner A. 2004. Monitoring of a paper mill wastewater treatment plant using UV/VIS spectroscopy. *Water Science and Technology*. 49(1): 9-14.

Lohrke J, Frenzel T, Endrikat J, Alves FC, Grist TM, Law M, Lee JM, Leiner T, Li K, Nikolaou K, Prince MR, Schild HH, Weinreb JC, Yoshikawa K, Pietsch H. 2016. 25 Years of Contrast-Enhanced MRI: Developments, Current Challenges and Future Perspectives. *Advances in Therapy*. 33(1): 1-28.

Mi P, Cabral H, Kokuryo D, Rafi M, Terada Y, Aoki I. 2013. Gd-DTPA-loaded polymeremetal complex micelles with high relaxivity for MR cancer imaging. *Biomaterials*. 34(2): 492-500.

Munshi K, Dey A. 1970. Spectrophotometric determination of lanthanides using 4-(2-Pyridylazo) resorcinol. *Mikrochimica Acta*. 59(5): 751-756.

Murata N, Gonzalez-Cuyar L, Murata K, Fligner C, Dills R, Hippe D, Maravilla K. 2016. Macrocyclic and other non-group 1 gadolinium contrast agents deposit low levels of gadolinium in brain and bone tissue: preliminary results from 9 patients with normal renal function. *Investigative Radiology*. 51(7): 447-453.

Ohyoshi E. 1984. Spectrophometric determination of formation constant of 1:1 complexes of lanthanides with 4-(2-pyridylazo)-resorcinol (PAR). *Talanta*. 31(12): 1129-1132.

Patel MU, Demir-Cakan R, Morcrette M, Tarascon JM, Gaberscek M, Dominko R. 2013. Li-S battery analyzed by UV/Vis in operando mode. *Communication*. 6(7): 1177-1181.

Ramalho J, Semelka R, Ramalho M, Nunes R, AlObaidy M, Castillo M. 2016. A gadolinium-based contrast agent accumulation and toxicity: an update. *American Journal of Neuroradiology*. 37(7): 1192-1198.

Rogosnitzky M, Branch S. 2016. Gadolinium-based contrast agent toxicity: a review of known and proposed mechanisms. *Biometals*. 29(3): 365-376.

Sabel CE, Shepherda JL, Siemann S. 2010. A direct spectrophotometric method for the

simultaneous determination of zinc and cobalt in metalloproteins using 4-(2-pyridylazo) resorcinol. *Analytical Biochemistry*. 391(1): 74-76.

Sherry AD, Caravan P, Lenkinski RE. 2009. Primer on gadolinium chemistry. *Journal of Magnetic Resonance Imaging*. 30(6): 1240–1248.

Wang YX, Schroeder J, Siegmund H, Idée JM, Fretellier N, Jestin-Mayer G, Factor C, Deng M, Kang W, Morcos SK. 2015. Total gadolinium tissue deposition and skin structural findings following the administration of structurally different gadolinium chelates in healthy and ovariectomized female rats. *Quantitative Imaging in Medicine and Surgery*. 5(4): 534-545.

Zhou Z, Lu ZR. 2012. Gadolinium-based contrast agents for MR cancer imaging. *Wiley Interdiscip Rev Nanomed Nanobiotechnol*. 5(1): 1-18.